*Journal of Statistical Physics, Vol 43, Nos. 3/4, 1986*

# Nonequilibrium Phase Transitions in Stochastic Lattice Systems: Influence of the Hopping Rates

**J. L. Vallés[1] and J. Marro[1]**

*Received December 6, 1985; final January 2, 1986*

Two-dimensional lattice-gas models with attractive interactions and particle-conserving hopping dynamics under the influence of a very large external electric field $\vec{E}$ along a principal axis are studied in the case of different ratios $\Gamma$ between the jump rates in the field direction and perpendicular to it using different transition probabilities. We investigate the dependence of the nonequilibrium steady-state properties on the transition mechanism. We find self-similarity with respect to $(T, \Gamma)$ and a coexistence curve critical exponent which, for small $\Gamma$, seems independent of $\Gamma$. There is some evidence that this exponent might be halfway between the equilibrium mean field and Onsager's values. A crossover toward mean-field behavior for large $\Gamma$ seems also identified.

**KEY WORDS:** Stochastic lattice-gas model, stationary nonequilibrium states; superionic conductors; hopping dynamics.

## 1. INTRODUCTION

The lattice-gas version of the Ising model with particle-conserving hopping dynamics under the influence of an external electric field can be used to model the so-called fast ionic or superionic conductors.[1] These are compounds such as AgI characterized by a sharp break in the slope of their conductivity-versus-temperature curve around some temperature (which can be below the melting point, depending on the nature of the interactions), by relatively large ionic conductivities above that temperature (so

Partially supported by the US-Spanish Cooperative Research Program, Grant CCB-8402025.

[1] Departamento de Fisica Teórica, Universidad de Barcelona, Diagonal 647, 08028 Barcelona, Spain.



0022-4715/86/0500-0441$05.00/0 

822/43/3-4-4

that they behave as solid electrolytes)[2] and, as a consequence, they have some promising technological applications.[3] In addition, this model is convenient for the analysis of "phase transitions" in stationary nonequilibrium states.[4]

Recent studies by Katz, Lebowitz, and Spohn[4] in two dimensions and by Marro *et al.*[5] in three dimensions have shown, for instance, that a very strong uniform electric field $\vec{E}$ along one of the principal axes of a lattice with periodic boundary conditions raises the critical temperature of the "ferromagnetic" (i.e., attractive interactions) Ising model, $T_c(E) > T_c(0)$ (the shift in $T_c$ is the opposite for "antiferromagnetic" (repulsive) interactions,[4] a case which will not be considered here). Moreover, there were some indications that this nonequilibrium phase transition might have a mean-field character. Namely, a numerical experiment for a three-dimensional system with n.n. interactions and large $E$[5] revealed that the coexistence curve critical exponent is larger than the equilibrium value $\beta \simeq \frac{5}{16}$ (perhaps $\beta = \frac{1}{2}$). If that is indeed the case, then this model would resemble the situation for a fluid under shear where it was predicted by Onuki and Kawasaki,[6] and consequently confirmed experimentally by Beysens and Gbadamassi,[7] that the corresponding gas–liquid phase transition has mean-field behavior.

The model has been analyzed by van Beijeren and Schulman[8] in the limit of an infinite ratio $\Gamma$ between the jump rates in the field direction and perpendicular to it. This variation on the model is interesting for two reasons. First, because it produces some kind of a quasi one-dimensional conduction which resembles the situation in some materials such as hollandite where $K^+$ ions are compelled to move in channels (See Ref. 9, and references therein). Second, because the critical exponents can in this case be found exactly,[8,10] unlike the case $\Gamma = 1$ where our present information comes mainly from numerical experiments.[4,5] In fact, they find that exponents are mean-field. The critical temperature and other details strongly depend on the choice for $\Gamma$ and on transition probabilities.[8,10]

It is the purpose of this paper to relate the phase transition found by Katz *et al.*[4] to the one described exactly by van Beijeren *et al.*[8,10] We study the crossover toward a quasi-one-dimensional situation, and analyze qualitatively the influence of the system evolution mechanism on the nature of those nonequilibrium phase transitions. To this end we investigated various two-dimensional stochastic models (like the one mentioned before) in strong fields. We used several $L \times K$ ($K = L$ and $K \ll L$) lattices half filled with particles with different transition probabilities and ratios $\Gamma$ for the microscopic mechanism of the evolution. We find how the latter influence the critical temperature, phase diagram, and other properties, and conclude some properties of the order-parameter exponent. We also find some

evidence that the critical behavior might be halfway between mean-field and Onsager equilibrium critical behavior, say $\beta \simeq 0.23$. This increases the interest in studying more thoroughly these and related models.

## 2. DESCRIPTION OF MODELS

The basic model of interest has already been described elsewhere.[4,5,8] It consists in the present case of a $L \times L$ square lattice whose sites can be either occupied by a particle (ion), represented by $n_i = 1$, or empty, $n_i = 0$; $i = 1, 2, \ldots, N = L^2$ denotes the lattice sites. The mean system density, $\rho = N^{-1} \sum_i n_i$, is set $\rho = \frac{1}{2}$. We also consider here quasi-one-dimensional $L \times K$ ($K \ll L$) lattices.

A given initial configuration $n_0 = \{n_i, i = 1, 2, \ldots, N(=L^2 \text{ or } LK)\}$ evolves according to a stochastic hopping dynamics with conserved $\rho$. Namely, particles hop to n.n. empty sites according to given transition probabilities implying the evolution of the system toward a "canonical" state at a prescribed temperature, in the sense that they satisfy an appropriate detailed balancing condition. We also assume the existence of an external uniform electric field $E\hat{x}$ along one of the principal directions of the periodic lattice, $\hat{x}$. This induces a preferential hopping in the direction $\hat{x}$ leading to a nonequilibrium steady state with a net steady current. This effect is enhanced here by considering a very strong field, $E \to \infty$, so that the jumps in the direction $-\hat{x}$ are practically forbidden. In addition, we also enhance the jumps in the direction of the field as compared to those perpendicular to it, in the directions $\pm \hat{y}$, by performing in some cases the former with a frequency $\Gamma$ times larger than the latter.

The evolution of the system has been analyzed in the case of different jump mechanisms which basically correspond, repectively, to the usual Metropolis[11] and Kawasaki[12] dynamics, in both cases, however, with the extra consideration of an external electric field and $\Gamma \geqslant 1$ and to the dynamics recently proposed by van Beijeren and Schulman[8] in the case of finite $\Gamma$. These jump mechanisms are implemented in the computer as follows.

Let us define the interaction energy as

$$H(\{n\}) = -4J \sum_{\text{n.n.}} n_i n_j, \qquad J > 0 \tag{1}$$

In the case of the jump *mechanism A*, the evolution proceeds by choosing at random a site $i$ and one of its n.n. sites $j$. The sampling for $j$ is performed with a frequency $\Gamma$ times larger in the $\pm \hat{x}$ directions than in the $\pm \hat{y}$ directions. When $(i, j)$ happen to be particle–particle or hole–hole states, the program increases the number of "attempted jumps," but no move is per-

formed. Otherwise, the attempted jump results in an actual move of the particle from $i$ to $j$ (or vice versa) with probability 1 when $\Delta H \pm E \leqslant 0$ and with probability $\exp[-(\Delta H \pm E)/k_B T]$ when $\Delta H \pm E > 0$. Here $\Delta H$ is the change in the energy (1) produced by the jump, and the signs $\pm$ hold, respectively, when it is attempted in the directions $\mp \hat{x}$ (note that $E = 0$ for jumps along $\pm \hat{y}$). This procedure can be seen to satisfy detailed balance locally.[4] The unit of time for the evolution *(MC step)* is the number of attempted jumps divided by $N$.

Note that for $\Gamma = \infty$ only jumps in the $\pm \hat{x}$ directions would occur so that the system can then be considered as a collection of Ising chains along $\hat{x}$, whose particles cannot hop between chains, although they interact when located at n.n. positions. The fact that the known solution for an Ising chain compels one to expect that the suppression of the interactions between neighboring chains would make $T_c(E) = 0$ indicates the interest to analyze different jump procedures.

The above mechanism, which is a straightforward generalization of the Metropolis transitions mechanism,[11] was also implemented in a few cases in a slightly different way, which shall be termed in the following as *mechanism A'*: A pair of n.n. sites $(i, i_x)$ is selected at random where $i_x$ represents a n.n. position of site $i$ in the $+\hat{x}$ or $-\hat{x}$ directions. The jump is performed (with probability 1) when the status at $(i, i_x)$ happens to be particle-hole and $i_x$ points in the $+\hat{x}$ direction; otherwise the attempt produces no move. This is repeated until one actually performs a given number $\Gamma'$ of actual jumps. Then new sites $(i, i_y)$, where $i_y$ indicates the n.n. position of site $i$ in the $+\hat{y}$ or $-\hat{y}$ directions, are selected at random until a particle-hole pair is found; the particle and the hole are then interchanged with probability 1 if $\Delta H \leqslant 0$ or with probability $\exp(-\Delta H/k_B T)$ otherwise. After these attempts in the direction perpendicular to the field, the cycle is started again and repeated as necessary. Each cycle requires $\Gamma \gg \Gamma'$ random selections of n.n. sites wich contribute to the Monte Carlo time; $\Gamma$ is defined as before. Note that the main difference between mechanisms $A$ and $A'$ is that the time intervals between jumps in $A$ are random whereas they are fixed in $A'$.

In order to study a really different transition mechanism with some physical relevance we also consider case A, but with transition probabilities given by $[1 + \exp(-(\Delta H \pm E)/k_B T)]^{-1}$ where $E = 0$ for jumps in the $\pm \hat{y}$ directions. This, which generalizes the usual Kawasaki's procedure,[12] will be termed *mechanism B*.

The transition mechanism considered by van Beijeren *et al.*[8,10] differs from those above. These authors make essentially the assumption (corresponding to $\Gamma = \infty$) that the particles along each line in the direction of the field "rapidly" return to a stationary condition between consecutive

jumps in the direction perpendicular to the field and consider a transition probability whose normalization is independent of $H$. One may in principle simulate directly such a condition by equilibrating, after a vertical jump, the two involved rows by randomly redistributing the given number of particles in each of the two rows. Our algorithm for this, however, drives the system very slowly toward the stationary state. Instead we approached that condition by *mechanism C* which reproduces case $A$ but with a transition probability which equals $\Gamma$ for jumps in the direction of the field and equals $\exp(-\Delta H/2k_BT)$, normalized to its maximum value, for jumps perpendicular to the field. This allows the study of finite values of $\Gamma$ and tends to the mechanism in Refs. (8, 10) in the limit $\Gamma \to \infty$.

## 3. DISCUSSION OF RESULTS

We describe here the results from a series of numerical experiments covering a broad range of temperatures which we measure in units of $T/T_c$; $T_c \equiv T_c(0) = 8J/k_B \sinh^{-1}(1)$ represents the Onsager (zero field, equilibrium) critical temperature. Most computations refer to $L \times L$ ($L = 50$, $N = 2500$) lattices; consequently we had to discard from the analysis of critical behavior the points very close to $T_c(E, \Gamma)$ affected by finite size effects, as we discuss later on. These square lattices are studied in the case of mechanism $A$ with $\Gamma = 1$, 5, 20, and 80, each for $T/T_c \cong 0.8$, 1.0, 1.1, 1.2, 1.3, 1.4, and 1.5 (corresponding, respectively, to $16J/k_BT = 2.203$, 1.763, 1.602, 1.469, 1.356, 1.259, and 1.175), and in the case of mechanism $A'$ with $\Gamma' = 80$ (requiring typically $\Gamma \gtrsim 400$) for several temperatures. In addition, we studied the influence of the transition mechanism on the stationary state by evolving $L \times K$ ($L = 10{,}000$, $K = 2$, $N = 20{,}000$) lattices via the jump mechanisms $A$, $B$, and $C$, the temperature ranging from $T/T_c = 0.05$ to $T/T_c = 5$.

Periodic boundary conditions are always assumed in order to minimize finite size effects and produce a steady current in the direction of the field. The field is always assumed effectively infinitely strong in the sense that no actual jumps in the $-\hat{x}$ direction occur; in the case where the value of the field appears explicitly in the transition probability, that was accomplished by putting $E = 15k_BT$ except at very low temperatures where $E = 75k_BT$ ($T/T_c \leqslant 0.5$) or $E = 125\,k_BT$ ($T/T_c = 0.05$) was required.

Given that we are only interested in the steady-state properties, the initial configuration $n_0$ for each run is chosen in such a way that the CPU computer time is minimized and one obtains the most reliable results compatible with the other conditions in our computations; e.g., we compared and averaged in some cases results coming from two different runs started at "infinite temperature" (random $n_0$) and at a temperature below $T$, the

characteristic one for that experiment, and we frequently used configurations obtained in previous runs. In any case, the system was allowed to evolve long enough (typically between $10^5$ and $10^6$ MC steps), until we were reasonably convinced that a stationary state had been reached, and we made about 150 measurements of the magnitudes of interest along an additional evolution, until good Gaussian distributions were obtained. This is much more than the usual statistics required for equilibrium Monte Carlo computations.

We first refer to the results for square $L \times L$ lattices and will describe the behavior of $L \times K$ ($K \ll L$) lattices in Section 3(vii).

### (i) Configurations

We have investigated the behavior with $T$, $\Gamma$, and transition mechanisms of the steady state. Below some critical temperature $T_c(E, \Gamma) > T_c$ the system always undergoes a phase transition by segregating into a dense fluid (particle-rich) phase and a vapor (particle-poor) phase. Unlike in thermal equilibrium, however, the fluid–vapor system is strongly anisotropic. Typical configurations are shown in Fig. 1; they are qualitatively similar for any value of $\Gamma$.

While the system configurations are always striplike in the $\hat{x}$ direction, as was also reported in previous studies,[4,5] the temporal evolution of the system requires a comment. The system is seen to evolve first toward a state with several well-defined strips (Fig. 1a), the number of strips being apparently size-dependent; e.g., $50 \times 50$ lattices half-filled with particles usually develop two strips, very early, as in Fig. 1a, which may last for 100,000 MC steps or more, while we observe up to 15 strips during short runs in a $300 \times 300$ lattice. The two-strip states seem stable although the system presents rather large, probably "anomalous" fluctuations. Eventually, typically well after 100,000 MC steps, the two strips come rather suddenly together to form one-strip states. In a few cases at the lowest temperatures this never happened during 300,000 MC steps or more, i.e., the two-strips state then persisted during our whole evolution, and we had to manipulate the system to create artificially one-strip configurations by moving together the existing strips. On the contrary, we never observed a one-strip state to split again into two strips.

It seems clear that one-strip states are the only stable ones under the present stationary conditions, i.e., finite $\Gamma$, n.n. interactions, and finite size of the system, in the sense that multistrip states would always decay sooner or later during such computer simulations. It seems to follow from the work by van Beijeren *et al.*,[8,10] however, that the relaxation time of multistrip stationary states diverges in the case $\Gamma \to \infty$, weak interactions per-

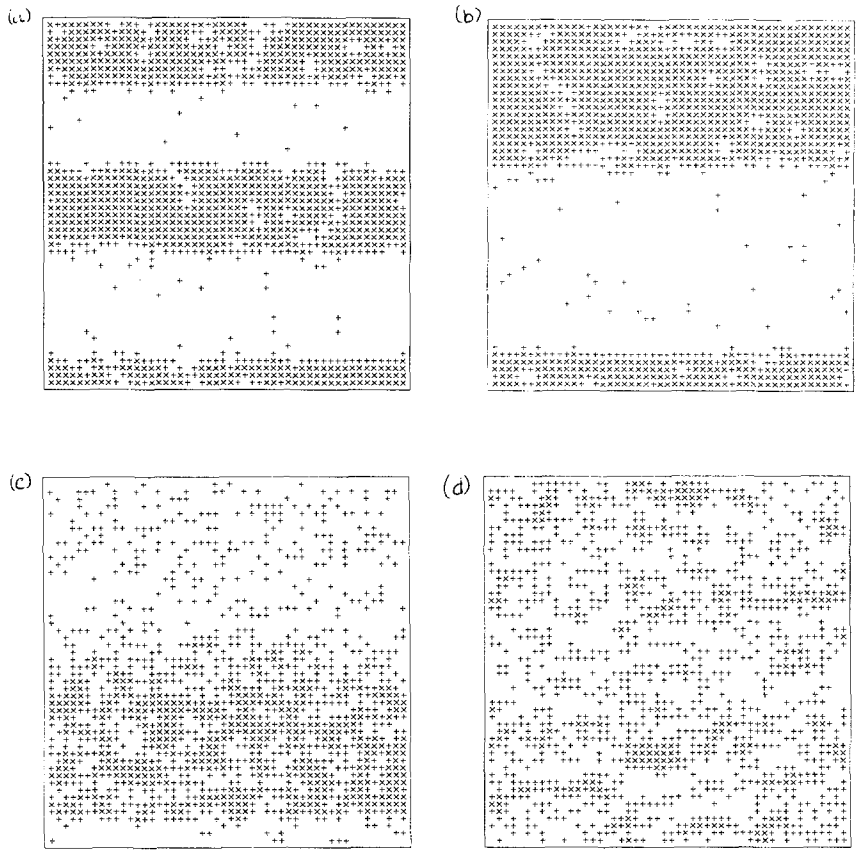


Fig. 1. Typical system configurations for a $50 \times 50$ lattice with periodic boundary conditions half-filled with particles under an "infinite" field $\vec{E}$ directed along the horizontal direction. Two different symbols are used in order to emphasize the interfaces shape and the clustering in the system: the crosses represent particles surrounded by particles at all the n.n. positions, while the pluses represent particles having at least one n.n. hole. (a) A two-strip configuration during the evolution of the system for $\Gamma = 5$ and $T = 0.8T_c(0)$ below $T_c(E, \Gamma)$. (b) A one-strip, stationary configuration for the same system as in (a). (c) A one-strip configuration for $\Gamma = 20$ and $T = T_c(0)$ below $T_c(E, \Gamma)$. (d) A configuration for $\Gamma = 1$ and $T = 1.5T_c(0)$ above $T_c(E, \Gamma)$ during the final stationary evolution.

pendicular to the field, and infinite system size. Our observations above thus correspond to a crossover toward such a situation. We should also point out that the mean values reported in the following for the order parameter, energy, etc., which correspond to one-strip states, are within the statistical fluctuations of the corresponding values for the metastable, intermediate two-strip states and that the only quantitative differences between

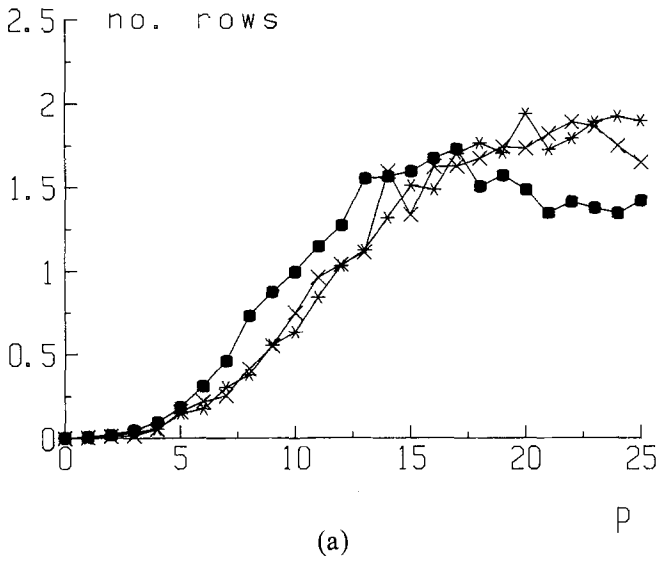


(a)

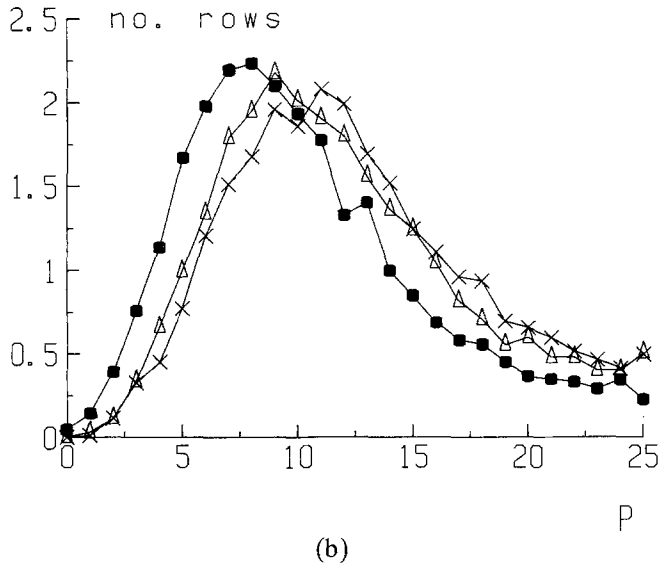


(b)

Fig. 2. Number of rows along the direction of the field which contain $p = 0, 1, 2, \ldots$, particles versus $p$. Because of symmetry only $p \leqslant 25 = N^{1/2}/2$ is shown. The symbols are as follows: $\Gamma = 1$ (asteriks), 5 (circles), 20 (crosses), 80 (pluses), and 400 (triangles). (a) Different cases above $T_c(E, \Gamma)$ showing approximately a similar behavior; they correspond to the states ($\Gamma = 1$, $T = 1.4T_c(0)$), ($\Gamma = 5$, $1.3T_c$), and ($\Gamma = 20$, $1.2T_c$). (b) Same as in (a) for the cases ($\Gamma = 5$, $1.1T_c$), ($\Gamma = 20$, $T_c$), and ($\Gamma = 400$, $0.8T_c$), below $T_c(E, \Gamma)$. (c) On the contrary, different values of $\Gamma$ at the same temperature, $T = 0.8T_c(0)$ in all cases, lead to very different states.

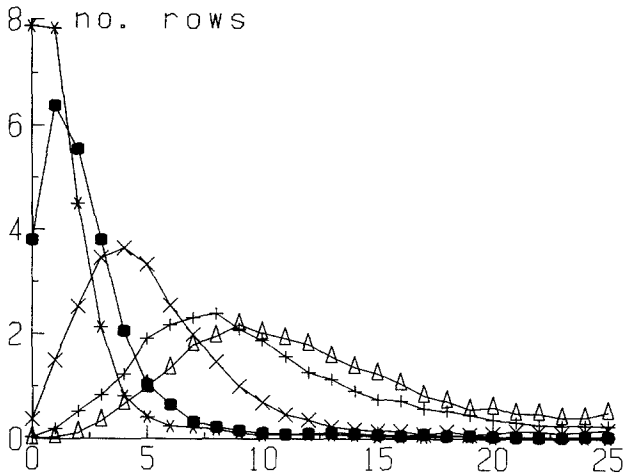


(c)

Fig. 2 (*continued*)

them seem to concern the fluctuations which are larger for two-strip intermediate states.

The final, one-strip system configurations can also be analyzed by looking at the graphs of Fig. 2, where we have plotted, for selected values of $T$ and $\Gamma$, the number of rows along the $\hat{x}$ direction which contain $p = 0, 1, 2, \ldots, L/2$ particles versus $p$. These graphs reveal that one may compare, for instance, the following $(T/T_c, \Gamma)$ states: (1.1, 5), (1.0, 20), and (0.8, 400), so that there is a kind of self-similarity in the steady state. This is confirmed by noting the clear differences shown by Fig. 2(c) between states at the same temperature, e.g. (0.8, 1), (0.8, 5), and (0.8, 20).

### (ii) Structure Function

More quantitative information follows from the analysis of the structure function which is defined as

$$S_{T,\Gamma}(\vec{k}) = N^{-1} \sum_{\vec{r} \in N} |e^{i\vec{k}\cdot\vec{r}} n(\vec{r})|^2 \tag{2}$$

where $\vec{k}$ runs over the first Brillouin zone. This is indeed highly anisotropic; see Table I showing some representative values of $S_{T,\Gamma}(k_x, k_y)$ near $\vec{k} = 0$ where one may again distinguish the situation above $T_c(E, \Gamma)$ from the one below it, apart from finite size effects which tend to obscure the situation very near $T_c(E, \Gamma)$. It also seems that the structure function

**Table I. Representative Values of the Ensemble Average of the Function $S_{T,\Gamma}(k_x, k_y)$[a]**

| | 0 | 1 | 2 | 3 | 4 | 5 |
|---|---|---|---|---|---|---|
| 0 | 0 | 920 | 0.2 | 99 | 0.2 | 34 |
| 1 | 0.2 | 0.2 | 0.2 | 0.2 | 0.2 | 0.2 |
| 2 | 0.1 | 0.2 | 0.2 | 0.2 | 0.2 | 0.2 |
| 3 | 0.1 | 0.1 | 0.1 | 0.2 | 0.2 | 0.2 |
| 4 | 0.1 | 0.1 | 0.1 | 0.1 | 0.1 | 0.2 |
| 5 | 0.1 | 0.1 | 0.1 | 0.1 | 0.1 | 0.1 |

(a)

| | 0 | 1 | 2 | 3 | 4 | 5 |
|---|---|---|---|---|---|---|
| 0 | 0 | 704 | 1.6 | 70 | 1.5 | 23 |
| 1 | 0.5 | 0.4 | 0.4 | 0.4 | 0.5 | 0.5 |
| 2 | 0.3 | 0.4 | 0.3 | 0.4 | 0.4 | 0.4 |
| 3 | 0.3 | 0.4 | 0.4 | 0.3 | 0.4 | — |
| 4 | 0.3 | 0.3 | 0.3 | 0.3 | — | — |
| 5 | 0.3 | 0.3 | 0.4 | — | — | — |

(b)

| | 0 | 1 | 2 | 3 | 4 | 5 |
|---|---|---|---|---|---|---|
| 0 | 0 | 367 | 4.1 | 17 | 3.7 | 12 |
| 1 | 0.7 | 0.8 | 0.8 | 0.7 | 0.6 | 0.7 |
| 2 | 0.7 | 0.6 | 0.8 | 0.7 | 0.6 | 0.7 |
| 3 | 0.7 | 0.6 | 0.7 | 0.8 | 0.8 | 0.7 |
| 4 | 0.6 | 0.7 | 0.6 | 0.7 | 0.6 | 0.7 |

(c)

| | 0 | 1 | 2 | 3 | 4 |
|---|---|---|---|---|---|
| 0 | 0 | 2 | 4 | 4 | 4 |
| 1 | 1.6 | 2.0 | 3.3 | 3.7 | 5.2 |
| 2 | 1.3 | 1.3 | 1.3 | 2.1 | 2.3 |
| 3 | 1.0 | 1.0 | 1.2 | 1.5 | 1.7 |
| 4 | 0.9 | 0.9 | 1.0 | 1.2 | 1.4 |

(d)

| | 0 | 1 | 2 | 3 | 4 |
|---|---|---|---|---|---|
| 0 | 0 | 45 | 11 | 1 | 7 |
| 1 | 1.1 | 1.0 | 1.2 | 1.3 | 1.2 |
| 2 | 1.1 | 0.9 | 1.0 | 0.9 | 1.0 |
| 3 | 1.0 | 0.9 | 0.8 | 0.9 | 1.0 |
| 4 | 0.9 | 1.1 | 0.9 | 0.8 | 0.9 |

(e)

| | 0 | 1 | 2 | 3 | 4 |
|---|---|---|---|---|---|
| 0 | 0 | 90 | 30 | 24 | 6 |
| 1 | 0.8 | 0.9 | 0.9 | 1.0 | 0.8 |
| 2 | 0.8 | 0.9 | 0.8 | 1.0 | 0.8 |
| 3 | 0.8 | 0.8 | 0.7 | 1.0 | 0.9 |
| 4 | 0.9 | 0.8 | 0.7 | 0.9 | 0.7 |

(f)

[a] Near $\vec{k} = 0$, where the structure is more pronounced. The horizontal entries represent times the factor $(50/2\pi)\,k_y$ (i.e., the direction perpendicular to the field) and the vertical entries represent times the factor $(50/2\pi)\,k_x$. Cases (a), (b), and (c) are all for $T = 0.8T_c$ and, respectively, for $\Gamma = 1$, 20, and 400. Case (d) is for $\Gamma = 1$ and $T = 1.5T_c(0)$. Case (e) is for $\Gamma = 20$ and $T = 1.2T_c(0)$, where finite size effects seem important. Case (f) is for $\Gamma \cong 400$ and $T = 0.95T_c(0)$.

parallel to the field is, except for $k_y = 0$, practically independent of $k$, this being perhaps more evident the greater $\Gamma$ is (thus recovering the condition discussed by van Beijeren *et al.*[8,10] for $\Gamma \to \infty$).

### (iii) Order Parameter

The natural order parameter for the phase transition can be defined as[5]

$$m = (\langle M_x^2 \rangle - \langle M_y^2 \rangle)^{1/2} \tag{3}$$

where $\langle\ \rangle$ denotes the ensemble average and

$$M_x^2 = \frac{1}{N^{1/2}} \sum_y \left[ \frac{1}{N^{1/2}} \sum_x (2n_{xy} - 1) \right]^2 \tag{4}$$

$$M_y^2 = \frac{1}{N^{1/2}} \sum_x \left[ \frac{1}{N^{1/2}} \sum_y (2n_{xy} - 1) \right]^2 \tag{5}$$

This is a measure of the density difference between fluid and vapor phases; at infinite temperature is $\langle M_x^2 \rangle = \langle M_y^2 \rangle$, which becomes zero for $N \to \infty$ and $m = 0$ while in the limit of zero temperature $\langle M_x^2 \rangle \to 1$, $\langle M_y^2 \rangle \to 0$, and $m \to 1$. The variation of $m^2$ with $T$ and $\Gamma$ is depicted in Fig. 3. This shows a clear change of $T_c(E, \Gamma)$ with $\Gamma$ which in the limit $E \to \infty$ can be estimated, together with the rest of the evidence in this paper, as $T_c(\infty, 1) \simeq 1.3\ T_c$ (which confirms the value by Katz *et al.*,[4] $T_c(\infty, 5) \simeq 1.2\ T_c$ and $T_c(\infty, 20) \simeq 1.1\ T_c$. Fig. 3 also seems to indicate that there is a change in the derivative $\partial m/\partial T$ when comparing, for instance,

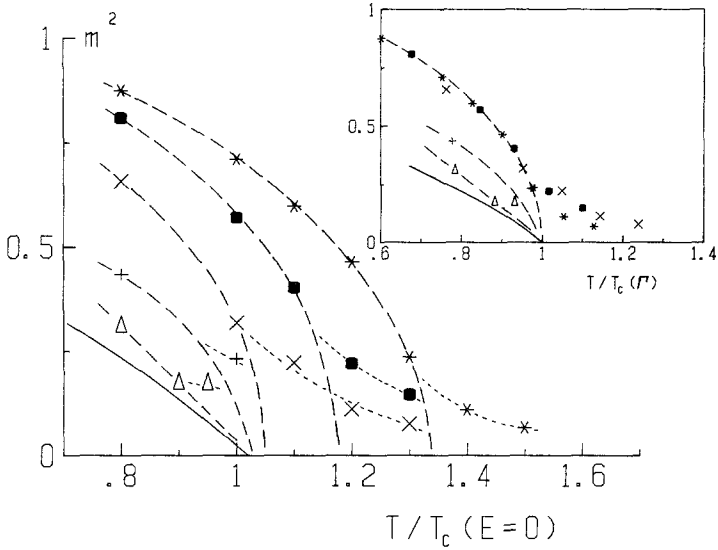


Fig. 3. The order parameter defined in Eqs. (3)–(5) (note that we are actually plotting $m^2$ for convenience) versus $T/T_c(0)$ for $\Gamma = 1$, 5, 20, 80, and $\sim 400$, respectively, from top to bottom (same symbols as in Fig. 2) in the case of squared $50 \times 50$ lattices. The dashed lines are only a guide to the eye; the dotted lines represent finite size effects; the solid line is the result $\Gamma \to \infty$ in Ref. 10. The inset shows the same data against $T/T_c(\Gamma)$ assuming $T_c(\Gamma \leqslant 20)$ as given by Table II and $T_c(80) = 1.03 T_c$, $T_c(400)$, $1.02 T_c$, $T_c(\infty) = 1.02 T_c$. The standard errors of the means imply error bars of the same height as the symbols used for $\Gamma \leqslant 80$ and larger by a factor 1.3 for $\Gamma \simeq 400$.

$\Gamma = 1$ with $\Gamma = 400$ (but not between the cases $\Gamma = 1$ and 5. The interpretation of our data for $\Gamma = 80$ and $\Gamma' = 80$ ($\Gamma \gtrsim 400$), which are also shown in Fig. 3, is more difficult than for the rest; we come to this point later on.

### (iv) Currents

The values for $T_c(\infty, \Gamma)$ can be estimated by analyzing the change with $T$ of bulk quantities with singularities at the critical temperature. One of them is the average current caused by the external field which probably presents smaller finite size effects severely affecting the estimation of $T_c(E, \Gamma)$. Moreover the average current, which is defined as the number of actual jumps performed in a given direction during the stationary evolution divided by its duration (in MC steps), behaves rather smoothly as a consequence of the averaging processes (over time and over all the particle-hole bonds parallel to the given direction) it includes. The current along the field direction, $J_x(\Gamma, T)$, is shown in Fig. 4 as a function of $T$ and $\Gamma$. As

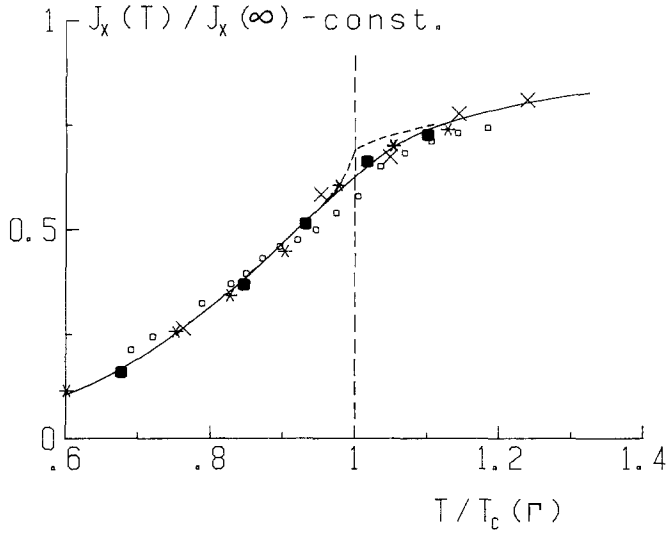


Fig. 4. Average saturation current divided by the corresponding value at infinite temperature versus $T/T_c(\Gamma)$ where $T_c(\Gamma)$ is given in Table II. Same symbols as in Fig. 2. For comparison we also included the values by Katz *et al.*[4] corresponding to $\Gamma = 1$ and to a smaller lattice, $30 \times 30$ (and poorer statistics); these are represented by small open circles. The solid line is a guide to the eye. The dashed curve suggests roughly the expected cusp at $T_c(\Gamma)$ which is here rounded off. Note that $\beta < \frac{1}{2}$ is suggested by the curvature shown by the data; a mean-field behavior would result in a line $J_x \propto \text{const} - (T_c - T)$. In order to emphasize that all the data for $\Gamma \lesssim 20$ follow a similar behavior, we plot $J_x(T)/J_x(\infty) - c(\Gamma)$ where $c(\Gamma = 1) = 0$, $c(\Gamma = 5) = 0.02$, and $c(\Gamma = 20) = 0.07$. The data for $\Gamma \geqslant 80$ seems to deviate from that behavior. Error bars here are always smaller than the height of the symbols used.

in the cases $\Gamma = 1$[4,5] and $\Gamma \to \infty$ (See Ref. 8) $J_x$ at intermediate values of $\Gamma$ increases with $T$, and one may relate $T_c(\Gamma)$ with a sudden break of the slope. The mean-field behavior found for $\Gamma \to \infty$ implies that $J_x$ is linear with $T$ near $T_c(\Gamma)$. This is approximately the case in Fig. 4; note, however, that most of the data reveal a curvature for $T < T_c(\Gamma)$ perhaps suggesting deviations from mean-field behavior.

## (v) Energy

The behavior of the energy along directions $\hat{x}$ and $\hat{y}$, measured as the number of particle-hole bonds per lattice site, $e_x$ and $e_y$, respectively, is shown in Fig. 5.

More interesting are the truncated n.n. correlations defined as the ensemble average of

$$g_x = 1 - [e_x(T)/e_x(\infty)] - M_x^2 \qquad e_x(\infty) = \tfrac{1}{2} \tag{6}$$

and

$$g_y = 1 - [e_y(T)/e_y(\infty)] \qquad e_y(\infty) = \tfrac{1}{2} \tag{7}$$

These are plotted in Fig. 6 as a function of $T$ for different values of $\Gamma$. The truncation by the square of the average density in each row reveals impor-

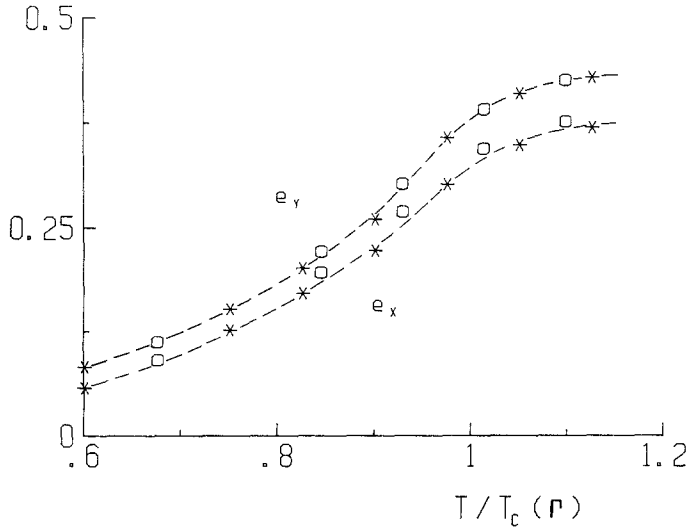


Fig. 5. The system energy parallel to the field ($e_x \propto J_x$) and perpendicular to the field ($e_y$), both measured as the number of particle-hole bonds per lattice site, versus $T/T_c(\Gamma)$ ($T_c(\Gamma)$ from Table II) for $\Gamma = 1$ (asterisks) and $\Gamma = 5$ (circles). Note that this behavior is very similar to that in Fig. 4. The data for $\Gamma \geqslant 20$ (not shown) follow a similar behavior except for displacements along the vertical axis. Error bars here are similar to those in Fig. 3.

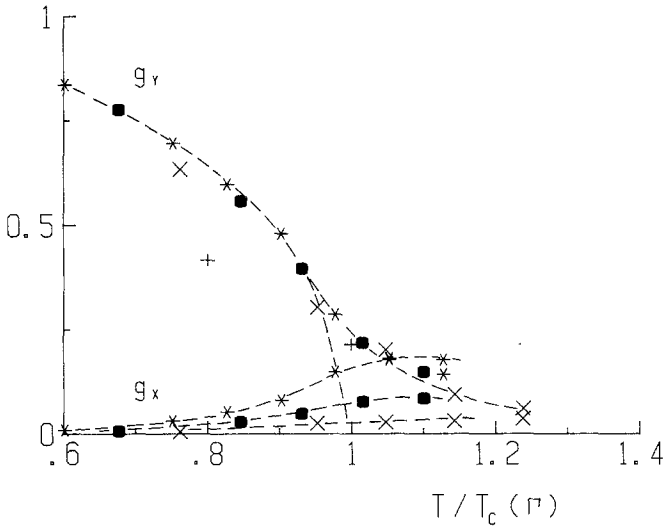


Fig. 6. Truncated nearest-neighbor correlation functions in directions parallel ($g_x$) and perpendicular ($g_y$) to the field versus $T/T_c(\Gamma)$ ($T_c(\Gamma)$ from Table II and $T_c(\Gamma=80)=1.03T_c$). Same symbols as in Fig. 2. The dashed lines guide the eye. Note the similar behavior between $g_y$ and $m$ in Fig. 3.

tant differences for the two principal directions: along $\hat{y}$ there is short-range order below $T_c(\Gamma)$ while this is suppressed along $\hat{x}$ because the field stirs the rows. One should expect this stirring to act more effectively with increasing $\Gamma$ and this is in fact supported by the data in Fig. 6. Note also that, as expected, the correlation along $\hat{y}$ at a given temperature increases with decreasing $\Gamma$.

### (vi) Critical Behavior

Our data for the order parameter seem accurate enough to allow a quantitative analysis of critical behavior, e.g. the corresponding distributions are very close to good Gaussians, and the critical, asymptotic region "$T \to T_c$" starts far below $T_c$, in two dimensions. Concerning the latter one should notice that mean-field formulas and Onsager's solution may lead, respectively, to $\beta = \frac{1}{2}$ and $\beta = \frac{1}{8}$ when making the usual log–log plots including a "critical" region as wide as $0.8 \leqslant T/T_c \leqslant 1$ (even wider in the case of mean-field behavior). As a consequence, we assumed that the data points shown in Fig. 3, excluding the ones affected by finite size effects (these are easily recognized by a comparison with previous MC data and by making plots such as the one in the inset of Fig. 3), belong to the critical region in this case. We then made plots of $\ln m$ versus

$\ln[1 - T/T_c(\Gamma)]$, trying to obtain the corresponding critical exponent, which we denote by $\beta$. Given that our estimations for $T_c(\Gamma)$ in the previous sections are not accurate enough for this purpose, we allowed ourselves to slightly modify $T_c(\Gamma)$ around the values quoted in Section (iii), looking for straight lines in the log–log plots. It became clear in this way that our data are not consistent with the equilibrium value $\beta = \frac{1}{8}$ not, apparently, with the mean-field value $\beta = \frac{1}{2}$: when one tries to demonstrate one of these values, the data systematically deviates from a linear behavior, both in the low and high temperature region within the considered range, and the values needed for $T_c(\Gamma)$ are manifestly inconsistent with the values reported above. Instead we can fit our data to the formula

$$m(T; \Gamma) = B(\Gamma)[1 - T/T_c(\Gamma)]^{-\beta} \tag{8}$$

with $\beta = 0.23 \pm 0.02$, roughly independent of $\Gamma$, and $T_c(\Gamma)$ consistent with Figs. 3–6 and the rest of the data. Table II lists the values obtained for $T_c(\Gamma)$ and $B(\Gamma)$ in this way; Fig. 7 depicts some graphical evidence.

The data for $\Gamma \geqslant 80$ can also be forced to follow the same behavior, i.e. $\beta \simeq 0.23$, by assuming $T_c(\infty, 80) \simeq (1.00 \pm 0.03)\, T_c$, $c(80) = -0.050$ and $T_c(\infty, \Gamma' = 80) \simeq (0.94 \pm 0.01)\, T_c$, $c(\Gamma' = 80) = -0.155$. While these values follow the trend shown by $\Gamma \leqslant 20$, they are inconsistent with a monotonous decrease of the function $T_c(\Gamma)$ and, simultaneously, with the exact result for $\Gamma \to \infty$ in the case of the mechanism considered in Ref. (10) (see Fig. 3). One may give several interpretations of this fact. First, the system evolution proceeded in the computer very slowly for $\Gamma \gtrsim 20$ so that our data for $\Gamma \geqslant 80$ are scarce and affected by larger error bars than the rest (see figure caption for Fig. 3). We think, however, that those data are still significant, so that this cannot be the only cause for the mentioned inconsistency. One

**Table II. Values for the Critical Temperature $T_c(E, \Gamma)$ and for the Parameter $c(\Gamma)$[a]**

| $\Gamma$ | $T_c(E, \Gamma)/T_c(0)$ | $c(\Gamma)$ | $\beta$ |
|---|---|---|---|
| 1 | $1.33 \pm 0.02$ | 0.142 | 0.226 |
| 5 | $1.18 \pm 0.02$ | 0.147 | 0.226 |
| 20 | $1.05 \pm 0.01$ | 0.114 | 0.225 |

[a] Gives the corresponding thermodynamic amplitude as $B(\Gamma) = \exp(c)$, needed to obtain the scaling behavior with $\Gamma$ shown by Fig. 7. The individual values for the critical exponent in Eq. (8) are also given; they are always around $\beta = 0.23$. The error bars reported state the limits for which the data follow a linear behavior as in Fig. 7 with $\beta = 0.23 \pm 0.02$ and values for $T_c(E, \Gamma)$ roughly consistent with the rest of the evidence in this paper.

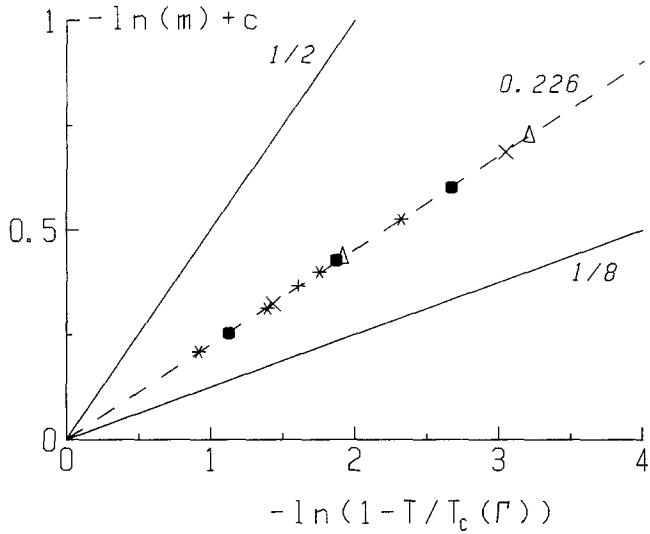


Fig. 7. Scaled log–log plot of the order parameter versus temperature (same data and symbols as in Fig. 3; the data affected there by finite size effects are not included here, however) in order to show that $\beta \approx 0.23$. The values for $c(\Gamma)$ and $T_c(E, \Gamma)$ used here are given in Table II (also $T_c(80) = T_c$, $c(80) = -0.050$, and $T_c(400) = 0.94 T_c$, $c(400) = -0.155$). The slopes $\frac{1}{2}$ (mean field) and $\frac{1}{8}$ (Onsager's) are also shown. The values in Ref. (10) for $\Gamma \to \infty$ lay on the $\frac{1}{2}$-line.

may also note that the cases $\Gamma = 80$ and $\Gamma \gtrsim 400$ were run, respectively, with mechanisms $A$ and $A'$, which basically differ from these studied by van Beijeren *et al.* We already know that the microscopic mechanism of evolution may influence the details of the phase transition (next section and Refs. (8, 10); for instance, preliminary data for a three-dimensional model system[14] seems to indicate that $T_c(\infty, \Gamma = 1)$ is very different, say, for mechanism $A$ than for mechanism $C$. Nevertheless, qualitative differences should probably tend to disappear as $\Gamma \to \infty$, so that again this is unlikely to produce by itself that apparent disagreement between theory and experiment. We thus believe that the most credible interpretation of this fact is that our data for $\Gamma \geqslant 80$ (and perhaps also the one for $\Gamma = 20$) are showing up a crossover from $\beta \simeq 0.23$ toward $\beta = \frac{1}{2}$, the mean-field behavior demonstrated for $\Gamma \to \infty$. As a matter of fact, $\Gamma \geqslant 80$ is indeed a very large value of $\Gamma$ in our $50 \times 50$ lattices and this interpretation seems also confirmed, for instance, by the situation in Figs. 3 and 6. Namely, the data for $\Gamma = 1, 5$ in those figures can be mapped onto a single curve, without having to scale the amplitudes (see Table II), by just scaling the temperature; the case $\Gamma = 20$ is ambiguous, and $\Gamma \geqslant 80$ clearly deviates from that curve.

### (vii) Rectangular Lattices

More information on the steady states of interest can be obtained by considering rectangular lattices $L \times K$. For instance, one should probably expect a well-defined nonequilibrium phase transition in quasi-one-dimensional lattices $K \ll L$ for large $L$ in the case of mean-field behavior. Also, these lattices may seem convenient in principle to study differences in the stationary state of the system caused by the transitions mechanism.

Thus we have analyzed the system $L = 10{,}000$ and $K = 2$ over a broad temperature range (from $T/T_c = 0.05$ to 5) in the case of the three transitions mechanisms, $A$, $B$, and $C$, described in Section 2. An "infinite field" acts in the direction of the largest dimension and periodic boundary conditions are assumed; the lattice is always half-filled with particles. In addition to the order parameter $m$ (3)–(5), the current along the field, and the energies $e_x$ and $e_y$, we have monitored now the following quantities

$$m' = (2\delta - 1)^{1/2} \tag{9}$$

where

$$\delta = \frac{1}{L} \sum_x (n_{x1} - n_{x2})^2 \tag{10}$$

and $n_{xy} = 0$, 1, and

$$\rho^* = n(1)^{-1}[n(1) - n(0) - n(2)] \tag{11}$$

where $n(p)$ represents the number of columns (perpendicular to the field) having $p$ particles; $p = 0$, 1 or 2 for the present model. A simple reasoning reveals that $m'$ and $\rho^*$ may vary between 1 and 0 when $T = 0$ and $T \to \infty$, respectively, for the kind of order one may expect, while the behavior of $m$ is perhaps more unpredictable in this quasi-one-dimensional case.

The corresponding behaviors with temperature are shown by Figs. 8 and 9 when $\Gamma = 1$ and $\Gamma = 20$. The resulting picture is rather simple: It seems that the sharp transition observed when $K \approx L$ is now absent for $K \ll L$, and that the data can be interpreted as revealing a "diffuse" phase transition with a broad changeover region $\Delta T_c$ such that $\Delta T_c$ would go to zero as $K \to L$ (for large enough values of $L$). The data for $m'$ and $e_y$, which are not shown in the figures, present a behavior similar to that for $\rho^*$ in Fig. 8.

When performing these computations we soon realized that, as expected, the system evolves extremely slowly at low temperatures, e.g. for $T < 1$, especially in the case of model $C$; as a consequence the data are then affected by large error bars. Otherwise we found no measurable differences with

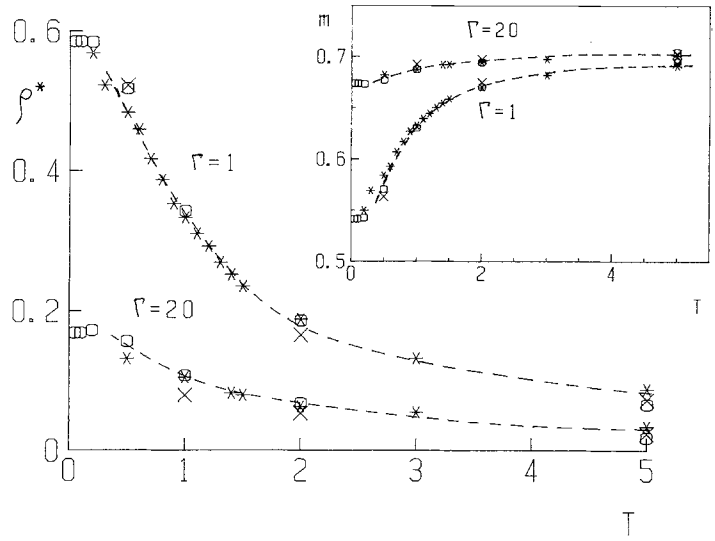


Fig. 8. The quantity $\rho^*$, as defined in Eq. (11), versus temperature (in units of the Onsager critical temperature for the square lattice) for $L \times K$ lattices, $L = 10{,}000$ and $K = 2$. Asterisks correspond to model $A$, circles to model $B$, and crosses to model $C$. The cases $\Gamma = 1$ and $\Gamma = 20$ are shown. The quantities $m'$ and $e_y$ present a behavior qualitatively similar to the one shown by $\rho^*$. The inset shows the behavior of $m$, as defined in Eqs. (3)–(5), versus temperature.

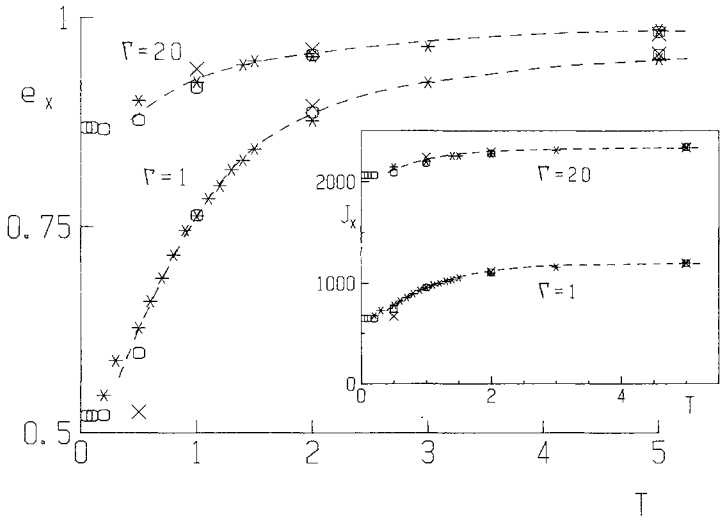


Fig. 9. The energy along the field direction versus temperature for $L \times K$ lattices. Same symbols as in Fig. 8. The inset shows the current along the field direction.

transitions mechanisms; it seems these will only appear within $\Delta T_c$ as $K \to L$. It is also noticeable that we do not observe qualitative differences between the cases $\Gamma = 1$ and $\Gamma = 20$; however, these differences will probably emerge as $\Gamma \to \infty$.

## 4. CONCLUSIONS

The lattice–gas version of the Ising model (two dimensions, square lattices, attractive interactions) with particle (ion) conserving ($\rho = 1/2$) hopping dynamics under the influence of a very large external electric field $\vec{E}$ along one of the principal axes is studied by MC methods in the case of different ratios $\Gamma$, $1 \leqslant \Gamma \gtrsim 400$, between the jump rates in the field direction and perpendicular to it, using some straightforward generalizations of the Metropolis mechanism. In addition, we also considered rectangular lattices ($L \times K$, $K \ll L$), with the field along the largest dimension, evolving toward the nonequilibrium stationary state with different mechanisms, namely some variations of the transition mechanisms first proposed, respectively, by Metropolis, Kawasaki, and van Beijeren–Schulman with $\Gamma = 1$ and 20. These mechanisms satisfy locally detailed balance conditions.

The nonequilibrium steady state of the system depends on transition mechanisms, value of $\Gamma$, and system shape. For $K = L$, that is, for square lattices, there is a critical temperature $T_c(\Gamma)$, which usually differs from the equilibrium one, such that for $T < T_c(\Gamma)$ the system orders in a very anisotropic phase. This is shown by the actual configurations of the system (Figs. 1), which are striplike parallel to the field, and more quantitatively by the structure function values (Table II). $T_c(\Gamma)$ is also characterized by a sudden break in the slope of the ionic current versus the temperature curve (Fig. 4).

States with several strips, the number of strips depending on the system size, may persist during the evolution below $T_c(\Gamma)$ for very long times (measured in MC steps) but they seem to decay finally into one-strip stationary states for finite $\Gamma$. In any case, the quantitative differences between the metastable multistrip states and the stable, stationary one-strip states seem rather small; e.g., the differences are within statistical fluctuations.[2]

Many properties of the final steady state change monotonically with $\Gamma$, e.g., the critical temperature for the nonequilibrium phase transition, $T_c(\Gamma)$, decreases with increasing $\Gamma$. The data for $\Gamma \geqslant 80$ seem consistent

[2] One should probably notice the fact that the order parameter for two-strip states in the $50 \times 50$ lattice leads to $\beta = 0.3$, instead of the value $\beta = 0.23$ we are reporting here for one-strip states, when the data is analyzed as described in Section 3(vi).

even with $T_c(\Gamma)$ becoming smaller than the Onsager's equilibrium critical temperature. This, however, is in conflict with $T_c(\Gamma \to \infty) \gtrsim T_c$ and seems to indicate that our data for large $\Gamma$ should be given an interpretation differing from that for small $\Gamma$, say $\Gamma \lesssim 20$, as we make precise later on.

We also find self-similarity of the steady-state $(T, \Gamma)$, as demonstrated in most figures throughout the paper. The most outstanding manifestation of this fact is contained in Fig. 7; that is, the order-parameter critical exponent is independent of $\Gamma$ for small $\Gamma$. The data for $\Gamma \lesssim 20$ also seem to allow the conclusion that $\beta \simeq 0.23$; this is halfway between the Onsager's equilibrium critical behavior and the typical mean-field behavior, which seems to characterize the exact case $\Gamma \to \infty$.[8,10] This result is also implied by the curvature shown by Fig. 4 below $T_c(\Gamma)$, which suggests that the current $J_x$ approaches $T_c(\Gamma)$ as const $-(T_c - T)^{2\beta}$ with $\frac{1}{8} \ll \beta \ll \frac{1}{2}$. Of course, more work on these and related models will be needed to make more precise the above conclusion and should this be the case, a good value of $\beta$ for "small" $\Gamma$. We are presently carrying out a finite-size scaling analysis with that aim.

The data for $\Gamma \geqslant 80$, on the other hand, is consistent with a crossover from the above behavior to the mean-field behavior shown by the case $\Gamma \to \infty$.[8,10] It is noticeable, however, that the limit $\Gamma \to \infty$ is reached very slowly in a computer simulation. For instance, the case $\Gamma \gtrsim 400$ ($\Gamma' = 80$), where the particles in a row of 50 sites along the field direction should practically equilibrate (in the sense of van Beijeren and Schulman[8] between two consecutive jumps perpendicular to the field, seems still "far" from the limiting case $\Gamma \to \infty$; this is supported, for instance, by Fig. 3 (where the data point corresponding to the highest temperature for $\Gamma' = 80$ is probably affected by finite size effects.) We also had noticeable difficulties in generating good Monte Carlo data for large $\Gamma$ due to the slow evolution of the system in the computer for $\Gamma \geqslant 80$.

We also investigate the case of quasi-one-dimensional lattices, $L \times K$, $K \ll L$. The sharp phase transition found for $K \approx L$ is absent in that case and no measurable differences are observed for small $\Gamma (\Gamma \leqslant 20)$ between models $A$, $B$, and $C$; this fact, as evidenced by Figs. 8 and 9, might suggest again that there is no mean-field behavior in the phase transition for small $\Gamma$ when $K \approx L$.

## ACKNOWLEDGMENTS

We would like to thank H. van Beijeren for correspondence and most valuable comments on a late version of the manuscript, and J. Krug, J. L. Lebowitz, H. Spohn, and Q. W. Zhang for helpful discussions and the communication of results prior to publication.

## REFERENCES


1. W. Dietrich, P. Fulde, and I. Peschel, *Adv. Phys.* **29**:527 (1980), and references therein.
2. T. Hibma, *Solid State Commun.* **33**:445 (1980).
3. J. B. Bates, J. Wang, and N. J. Dudney, *Phys. Today*, 09:46 (1980).
4. S. Katz, J. L. Lebowitz, and H. Spohn, *Phys. Rev.* **B28**:1655 (1983); *J. Stat. Phys.* **34**:497 (1984).
5. J. Marro, J. L. Lebowitz, H. Spohn, and M. H. Kalos, *J. Stat. Phys.* **38**, 725 (1985).
6. A. Onuki and K. Kawasaki, *Ann. Phys.* (N.Y.) **121**:456 (1979); **131**:217 (1981).
7. D. Beysens and M. Gbadamassi, *Phys. Rev.* **A22**:2250 (1980).
8. H. van Beijeren and L. S. Schulman, *Phys. Rev. Lett.* **53**:806 (1984).
9. I. Bernasconi, H. U. Beyeler, S. Strässler, and S. Alexander, *Phys. Rev. Lett.* **42**:819 (1979).
10. J. Krug, J. L. Lebowitz, H. Spohn, and Q. W. Zhang, to be published.
11. N. Metropolis, A. W. Rosenbluth, M. M. Rosenbluth, A. H. Teller, and E. Teller, *J. Chem. Phys.* **21**:1087 (1953).
12. K. Kawasaki, in *Phase Transitions and Critical Phenomena*, vol. 2, C. Domb and M. S. Green, eds. (Academic Press, London, 1972), pp. 443–501.
13. J. Marro *et al.*, unpublished results.